DOI: 10.1002/ejic.200700650

A Simple Non-Aqueous Route to Anatase TiO_2

Dong Jiang,[a,b] Yao Xu,*[a] Bo Hou,[a] Dong Wu,[a] and Yuhan Sun*[a]

Keywords: Titanium dioxide / Nonaqueous synthesis

High-yield nanocrystalline TiO_2 was successfully synthesised using a simple one-step procedure in a non-aqueous system. The synthesis was carried out in a teflon-lined autoclave at a temperature as low as 100 °C using titanium *n*-butoxide (TB) and acetic acid (AcOH) as starting materials without any co-solvent/additive. The thus formed TiO_2 was highly crystallised anatase TiO_2. The possible formation mechanism was also proposed based on the FTIR spectra recorded during the various reaction stages. The synthetic method explored in this study might contribute to the preparation of other metal oxides.

Introduction

Nanocrystalline TiO_2 particles have been intensively studied because of their widespread applications in many fields such as optics,[1] catalysis,[2] photocatalysis,[3] dye-sensitised solar cells,[4] gas sensors[5] etc. These applications of TiO_2 generally depend on the crystal structure of TiO_2. Among the three naturally occurring crystalline forms of TiO_2 (anatase, brookite and rutile), rutile is the most stable phase, whereas anatase has superior optoelectronic and photochemical properties.[6] The exploration of a simple and effective synthetic strategy for anatase TiO_2 should, therefore, be expected to attract a great deal of scientific and technological interest.

There have been a number of recent reports on the preparation of nanoscale anatase TiO_2. Among the various synthetic routes, the most general and versatile solution-phase synthetic strategy is based on the hydrolysis and condensation of titanium alkoxides or halides to create nanosised anatase TiO_2. Owing to the extreme moisture sensitivity of the titanium precursors, the directly hydrolytic process could not be controlled sufficiently. Later, it was found that carboxylic acids such as oleic acid and acetic acid used as chelating ligands could stabilise the high-reactivity titanium precursors and bring about the controllability of the hydrolysis and condensation process.[7,8] However, in most cases, these procedures were conducted at low temperature and yielded amorphous TiO_2 and subsequent hydrothermal processing[9–11] or calcination was necessary to induce crystallisation.[12,13]

To overcome the specific difficulties of aqueous systems, non-aqueous systems for the preparation of anatase TiO_2 have been developed, mainly including hydrolytic[14–17] and nonhydrolytic[18–26] strategies in non-aqueous media. Among these methods, the former hydrolytic route usually utilises carboxylic acid as ligands to stabilise the titanium precursors but some co-solvents/additives such as alcohols were also necessary to synthesise TiO_2 in those cases.[16,27–29] The latter, non-hydrolytic method was preferred for producing highly crystalline anatase.[20] The main non-hydrolytic routes involve the elimination reaction between titanium tetrachloride and oxygen donor molecules such as titanium alkoxides and organic ethers.[18–20] However, the elimination reactions used could produce environmentally unfavourable and volatile alkyl chlorides.[18–24] Therefore, it is necessary to explore a new synthetic route to anatase TiO_2 to avoid the problems encountered in conventional aqueous or non-aqueous syntheses.

Herein, we report an environmentally benign and simple method for synthesising anatase TiO_2 nanoparticles using only titanium *n*-butoxide (TB) and acetic acid (AcOH) as reactants. Although the reaction between AcOH and TB has been investigated in earlier research,[7,8,30] those studies were limited to investigating the solution chemistry between AcOH and TB. These days, the preparation of TiO_2 nanocrystals using AcOH and TB is seldomly reported. In the present work, we found AcOH reacts directly with TB to form the well-crystallised TiO_2 nanoparticles by solvothermal treatment at 100 °C, without the addition of any co-solvent and additive. Highly pure anatase TiO_2 was produced with a high yield of 95%.

[a] State Key Laboratory of Coal Conversion, Institute of Coal Chemistry, Chinese Academy of Sciences,
Taiyuan 030001, China
Fax: +86-351-4041153
E-mail: xuyao@sxicc.ac.cn
[b] Graduate University of the Chinese Academy of Sciences,
Beijing 100049, China

Supporting information for this article is available on the WWW under http://www.eurjic.org or from the author.

Results and Discussion

As shown in the XRD patterns of 100HAT2, 100HAT4 and 100HAT6, the diffraction peaks can be indexed to the (101), (004), (200), (105) and (211) crystal planes of TiO_2 (JCPDS File NO. 21–1272) (Figure 1, a). All the peaks can be assigned to the pure anatase phase and no peaks for other crystal types can be observed, suggesting the simplex crystal phase and high purity of the samples. It is a good feature that the well-crystallised TiO_2 particles can be synthesised at such a low reaction temperature of 100 °C. Significantly, the diffraction peak intensity of 100HAT4 is the strongest among those samples (Figure 1, a). Thus, it is believed that the molar ratio of AcOH:TB = 4:1 is optimal for synthesising well-crystallised anatase TiO_2. The average crystallite size of 100HAT4 is about 9 nm as estimated from the (101) diffraction peak using the Scherrer equation.[31] Part b of Figure 1 shows the XRD patterns of 100HAT4, 140HAT4, 180HAT4 and 220HAT4. In part b, with increasing solvothermal temperature, the intensities of the anatase TiO_2 diffraction peaks increase and the width of the (101) peak becomes narrower which is due to the improvement of crystallisation and growth of the crystallites. Consequently, the higher synthetic temperatures can lead to higher crystallinity and larger crystals in the range from 100–220 °C.

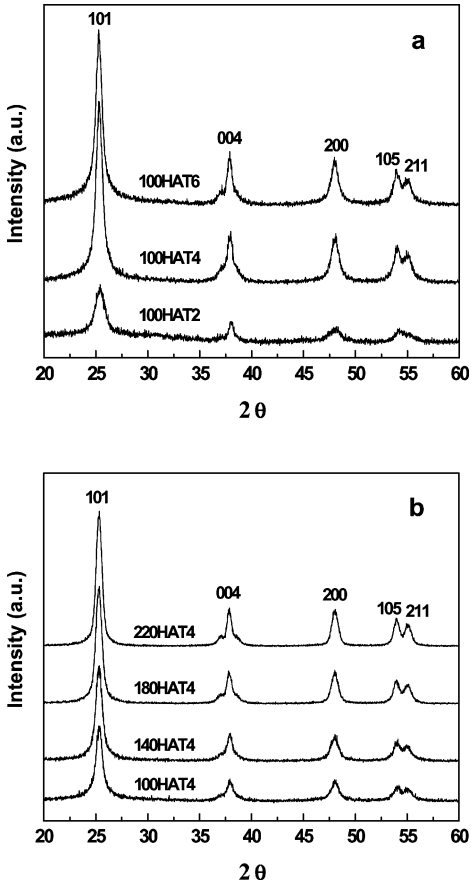

Figure 1. XRD patterns of (a) 100HAT2, 100HAT4 and 100HAT6; (b) 100HAT4, 140HAT4, 180HAT4 and 220HAT4.

Representative TEM images of 100HAT4 are showed in Figure 2. The sizes and shapes of the nanoparticles are not very uniform and some weak aggregation among the particles can be observed (Figure 2, a). The average particle size was estimated to be about 9 nm, in agreement with the crystallite size obtained from XRD. The HRTEM image of the 100HAT4 so obtained clearly reveals only the fringes of the (101) planes of anatase TiO_2 with a lattice spacing of about 0.35 nm (Figure 2, b). It is reasonable to believe that the TiO_2 nanopaticles are well-crystallised single crystal particles. The selected area electron diffraction (SAED) pattern is shown in Figure 2 (c). Detailed analysis indicates that the first diffraction circle in the pattern corresponds to the (101) plane. It should be noted that the nanoparticles are so small that the SAED pattern can not be taken from any individual nanoparticle in our TEM observation. Therefore, the diffraction spots can not be observed and only the diffraction circles are obtained.

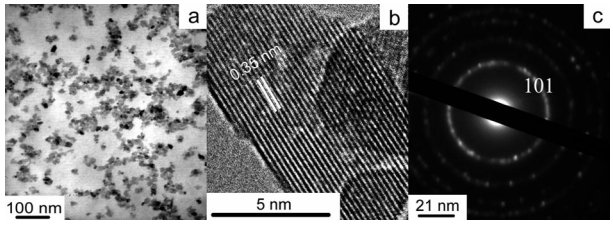

Figure 2. (a) TEM image of the sample of 100HAT4, (b) a high-resolution TEM image of the sample and (c) selected area electron diffraction pattern.

Raman spectra (Figure 3) of TiO_2 samples (100HAT2, 100HAT4 and 100HAT6) reveal five Raman bands at 147, 198, 398, 517 and 639 cm^{-1} ranging between 100 and 800 cm^{-1}. All the Raman peaks can be assigned to the E_g, E_g, B_{1g}, A_{1g} and E_g modes of the anatase phase of TiO_2, respectively,[32,33] and no peaks of any impurity can be observed. This result shows the good quality of the synthesised anatase TiO_2 and is in good agreement with the XRD results. It can be seen that the strongest peak at 147 cm^{-1} shows some shift towards higher wavenumbers compared with the 143 cm^{-1} from the reference data.[34] The blue shift may be the result of the quantum size effects and organic compounds chelated with the Ti atom.[35] After the synthesised TiO_2 samples were calcined at 400 °C for 4 h, no blue

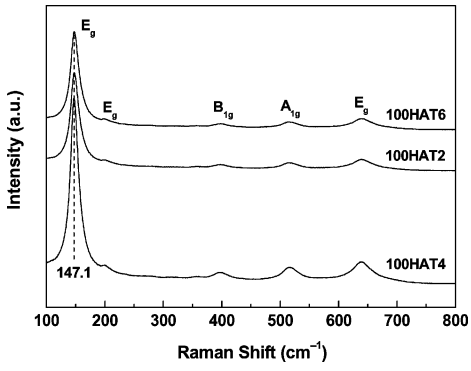

Figure 3. Raman spectra of 100HAT2, 100HAT4 and 100HAT6.

shift relative to 143 cm^{-1} could be observed in the Raman spectra due to the disappearance of the organic compounds. This is confirmed by the following TGA spectrum and the increasing TiO_2 particles size.

The TGA spectrum of 100HAT4 recorded under a flow of air (Figure 4) indicates two weight-loss stages in the temperature ranges of 30–100 °C and ca. 100–400 °C. The first weight loss (ca. 1.1%) corresponds to adsorbed water and organic molecules on the sample surface. The second large weight loss of about 10.9% is associated with the removal of organic compounds (e.g. CH_3CO_2nBu, boiling point 126 °C) derived from the synthetic process and the degradation of organic groups[8] contained in the final product. Above 400 °C, the weight of the 100HAT4 sample remains almost constant. Therefore, it can be postulated that the synthesised 100HAT4 sample after being calcined at 400 °C is absolutely pure TiO_2 without any organic impurities.

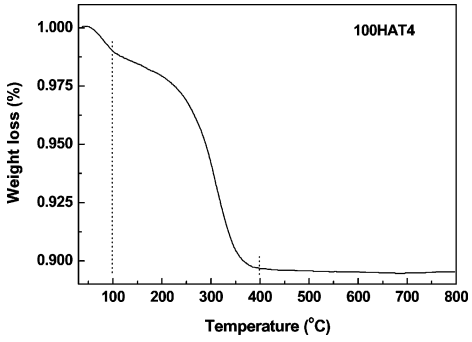

Figure 4. The TGA spectrum of the synthesised 100HAT4.

To understand the detailed reaction process between AcOH and TB, the FTIR spectra of AcOH, TB and the mixture of AcOH and TB are shown in parts a–c of Figure 5. Part c shows the FTIR spectrum recorded on the clear solution obtained by adding 4 mol AcOH per mol of TB with stirring for 30 min. Compared with parts a and b, some new bands can be observed at 3360, 1750, 1566, 1532, 1450, 1426 and 1292 cm^{-1} (Figure 5, c). In part c, the peaks around 1400–1500 cm^{-1} can be attributed to acetate ligands.[8,28,36] It is well known that the acetate ligands generated by the reaction of AcOH with TB have several modes of coordination, including monodentate and bidentate (chelating and bridging). The alcohol *n*BuOH is also generated as a by-product in the process of the formation of acetate ligands.[28,37] The frequency separation ($\Delta\tilde{\nu}$ = 140 cm^{-1}) between 1566 and 1426 cm^{-1} suggests that some acetate groups acts as bridging ligands. The frequency separation ($\Delta\tilde{\nu}$ = 82 cm^{-1}) between 1532 and 1450 cm^{-1} suggests that some other acetate groups are bonded as chelating ligands.[8,28,36] From Figure 5 (c) it is difficult to say whether a part of acetate groups act as monodentate ligands although the peak at 1714 cm^{-1} and the shoulder at 1292 cm^{-1} imply the existence of monodentate coordination. The newly emerged peak at 3360 cm^{-1} should be attributed to the stretching vibration of the hydroxy groups of *n*BuOH. Additionally, a slight increase in the intensity of the 1251 cm^{-1} band (C–O stretching of $CH_3COOnBu$), comparing parts a and c of Figure 5, suggests that CH_3COO is formed by an esterification reaction between *n*BuOH and the excess AcOH. Through the above FTIR analysis, it can be concluded that acetate ligands have been generated after the mixing AcOH with TB for 30 min but no FTIR characterised peak corresponding to Ti–O–Ti groups can be found.

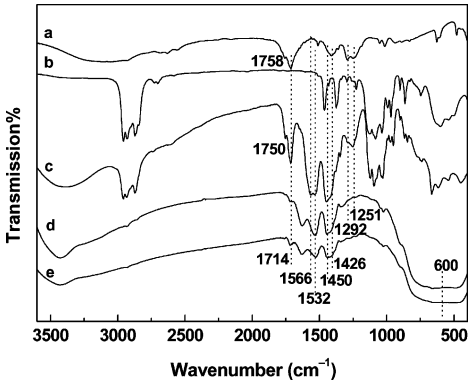

Figure 5. FTIR spectra of (a) AcOH, (b) pure TB, (c) the mixture of AcOH and TB with a molar ratio of 4:1 after 30 min at room temperature and FTIR spectra of the prepared xerogel from the mixtures after being solvothermally treated at 100 °C for (d) 2 h, (e) 12 h.

For the purpose of tracking the formation process of TiO_2, the FTIR spectra of the xerogels obtained after solvothermal reaction times of 2 h and 12 h at 100 °C are shown in Figures 5 (d and e). Compared with part c, a clear broad and strong band at 600 cm^{-1} can be observed in parts d and e, which can be assigned to the vibration of the Ti–O–Ti moiety of the titanium oxide network, suggesting the formation of TiO_2. Simultaneously, the absorption bands of the acetate ligands at 1714, 1566, 1292 cm^{-1} disappear indicating that the monodenetate and bridging ligands have transformed into the structure of Ti–O–Ti by a ploycondensation reaction.[27] It must be pointed out that the bands of the chelating ligand at 1532 and 1448 cm^{-1} are still visible even after 12 h of solvothermal treatment although their intensities decrease with an increase in the reaction time. It is also reasonable because the chelating ligand is very stable and still exists in the final product[8] which is consistent with the Raman and TGA results.

In addition, after the mixture with a molar ratio of AcOH/TB = 4 was solvothermally treated for 12 h, the liquid product was collected and characterised by GC. The detailed GC results are listed in Table 1. As shown in Table 1, it is clear that CH_3CO_2nBu is a dominant component in the produced liquid sample. Additionally, little water and unreacted CH_3CO_2H were detected.

Based on the above-mentioned analyses, a possible mechanism for the formation of TiO_2 can be proposed. Firstly, AcOH may react with TB to produce acetate ligands: $(CH_3CO_2)_xTi(nBuO)_{4-x}$, concomitant with the release of *n*BuOH; see Equation (1). The *n*BuOH formed during the former process of equation 1 could then react with

Table 1. The components and content of a liquid sample.

Component[a]	CH_3CO_2nBu	AcOH	H_2O
% Content[b]	95.56	2.66	1.58

[a] The component was confirmed by comparison of the retention times with those of a corresponding reference standard sample. [b] the content was determined using ethyl acetate as an internal standard.

unreacted AcOH to form water by a slow esterification reaction; see Equation (2). The water produced in Equation (2) can then react with both the acetate ligands and TB to generate Ti–OH and, subsequently, Ti–O–Ti bonds would be formed by a hydrolysis–condensation process. In Equation (3), the $R_xTi(n\text{BuO})_{4-x}$ is used to denote the acetate ligands and TB for convenience, where the "R′" represents CH_3CO_2– and *n*BuO–, respectively. Although the hydrolytic-condensation is the main process, the possibility of the acetate ligands $(CH_3CO_2)_xTi(OBu)_{4-x}$ also generating Ti–O–Ti bonds by nonhydrolytic condensation [Equation (4)] and finally forming TiO_2 cannot be ruled out[27] During the whole reaction process, CH_3CO_2nBu can be produced according to Equations (2) and (4) and therefore clearly be the primary by-product which is consistent with the former results. Consequently, the TiO_2 formation mechanism in our study may include both a hydrolytic–condensation and a nonhydrolytic–condensation process. Further investigations are in progress.

$$x\,CH_3CO_2H + Ti(n\text{BuO})_4 \longrightarrow (CH_3CO_2)_xTi(n\text{BuO})_{4-x} + x\,n\text{BuOH} \quad (1)$$

$$n\text{BuOH} + CH_3CO_2H \longrightarrow CH_3CO_2n\text{Bu} + H_2O \quad (2)$$

$$R_xTi(n\text{BuO})_{4-x} + H_2O \longrightarrow R_x(n\text{BuO})_{3-x}TiOH + n\text{BuOH}$$

$$R_x(n\text{BuO})_{3-x}TiOH + R_x(n\text{BuO})_{3-x}TiOR' \longrightarrow$$

$$R_x(n\text{BuO})_{3-x}\mathbf{Ti–O–Ti}R_x(n\text{BuO})_{3-x} + R'OH$$

$$R = n\text{BuO}, -OCCH_3;\ R' = H, n\text{Bu} \quad (3)$$

$$m\,(CH_3CO_2)_xTi(On\text{Bu})_{4-x} \longrightarrow$$

$$m/2\,[(CH_3CO_2)_{2x-1}\mathbf{Ti–O–Ti}(On\text{Bu})_{7-2x}] + m/2\,CH_3CO_2n\text{Bu} \quad (4)$$

Conclusions

In conclusion, a facile and green nonaqueous route was successfully developed to synthesise anatase TiO_2 at low temperature. The optimum molar ratio for obtaining crystalline TiO_2 is AcOH/TB = 4. The formation mechanism of TiO_2 should involve hydrolytic condensation and nonhydrolytic condensation during the reaction process. Moreover, this synthetic method could be extended further for the preparation of other oxide nanocrystals e.g. ZrO_2 (see electronic supporting information).

Experimental Section

General: Anatase nanocrystals were prepared using TB (> 98%, Alfa Aesar) and AcOH (> 99.5%, Tianjin Reagent Company) as starting materials. AcOH was distilled before use. The pipettes and autoclaves were dried before use. All the experimental operations were carried out under nitrogen. In a typical synthesis, TB (13.6 mL, 0.04 mol) and AcOH (9.2 mL, 0.16 mol) were mixed in a dry flask. The mixture was stirred for a further 30 min at room temperature. The resultant solution was then transferred into a Teflon-lined stainless autoclave and solvothermally treated at 100 °C for 12 h. After being left to cool to room temperature, the resultant off-white opaque monolith was washed three times with absolute ethanol. The products were dried at 60 °C under vacuum and ground into white powders. The yield was around 95% (approximately 3.05 g after being calcined at 400 °C for 4 h). The obtained TiO_2 sample was designated as *X*HAT*Y*, where *X* represents the solvothermal temperature and *Y* indicates the molar ratio of AcOH to TB.

The crystalline phases of the samples were characterised by X-ray powder diffraction (XRD, Cu-K_α, 40 kV, 40 mA, D8, Advance Bruker Axs). The morphology of the powder sample was observed by transmission electron microscopy (TEM, Hitachi-600-2) and high-resolution transmission electron microscopy (HRTEM, JEOL2010). Raman spectra were recorded with a Jobin–Yvon Labram HR800 spectrometer. The chemical structure information of the particles was obtained from FTIR spectra (Nicolet 470 Spectrometer). The TGA spectrum was recorded out on a NETZSCH STA 449C instrument under air from room temperature to 800 °C at a heating rate of 10 °C min^{-1}. The components of the final liquid samples were analyaed on a TCD gas chromatograph (Shimadzu GC-8A) equipped with a 3 m × 3.2 mm packed column of Carbowax 20 M on Chromosorb WAW 80/100 and argon as carrier gas.

Supporting Information (see also the footnote on the first page of this article): Preparation of ZrO_2 nanocrystals.

Acknowledgments

The financial support from the National Natural Science Foundation (No. 20573128), National Basic Research Program of China (No. 2005CB221402), and Shanxi Natural Science Foundations (No. 20051025, No. 2006021031 and No.2007021014) is acknowledged.

[1] K. L. Frindell, M. H. Bartl, A. Popitsch, G. D. Stucky, *Angew. Chem. Int. Ed.* **2002**, *41*, 959–962.
[2] W. J. Stark, K. Wegner, S. E. Pratsinis, A. Baiker, *J. Catal.* **2001**, *197*, 182–191.
[3] Z. B. Zhang, C. C. Wang, R. Zakaria, J. Y. Ying, *J. Phys. Chem. B* **1998**, *102*, 10871–10878.
[4] B. I. Lemon, J. T. Hupp, *J. Phys. Chem. B* **1999**, *103*, 3797–3799.
[5] D. Morris, R. G. Egdell, *J. Mater. Chem.* **2001**, *11*, 3207–3210.
[6] U. Diebold, *Surf. Sci. Rep.* **2003**, *48*, 53–229.
[7] S. Doeuff, M. Henry, C. Sanchez, *Mater. Res. Bull.* **1990**, *25*, 1519–1529.
[8] S. Doeuff, M. Henry, C. Sanchez, J. Livage, *J. Non-Cryst. Solids* **1987**, *89*, 206–216.

[9] A. Chemseddine, T. Moritz, *Eur. J. Inorg. Chem.* **1999**, 235–245.
[10] H. Yin, Y. Wada, T. Kitamura, T. Sumida, Y. Hasegawa, S. Yanagida, *J. Mater. Chem.* **2002**, *12*, 378–383.
[11] X. Yang, H. Konishi, H. Xu, M. Wu, *Eur. J. Inorg. Chem.* **2006**, 2229–2235.
[12] C. C. Wang, J. Y. Ying, *Chem. Mater.* **1999**, *11*, 3113–3120.
[13] H. Zhang, M. Finnegan, J. F. Banfield, *Nano Lett.* **2001**, *1*, 81–85.
[14] M. J. MqYunoz-Aguado, M. Gregorkiewitz, A. Larbot, *Mater. Res. Bull.* **1992**, *27*, 87–97.
[15] L. Laaziz, A. Larbot, A. Julbe, C. Guizard, L. Cot, *J. Solid State Chem.* **1992**, *98*, 393–403.
[16] C. Wang, Z. Deng, Y. Li, *Inorg. Chem.* **2001**, *40*, 5210–5214.
[17] A. Vioux, *Chem. Mater.* **1997**, *9*, 2292–2299.
[18] T. Trung, C. S. Ha, *Mater. Sci. Eng. C* **2004**, *24*, 19–22.
[19] P. Arnal, R. J. P. Corriu, D. Leclercq, P. H. Mutin, A. Vioux, *Chem. Mater.* **1997**, *9*, 694–698.
[20] T. J. Trentler, T. E. Denler, J. F. Bertone, A. Agrawal, V. L. Colvin, *J. Am. Chem. Soc.* **1999**, *121*, 1613–1614.
[21] M. Niederberger, M. H. Bartl, G. D. Stucky, *Chem. Mater.* **2002**, *14*, 4364–4370.
[22] H. Parala, A. Devi, R. Bhakta, R. A. Fischer, *J. Mater. Chem.* **2002**, *12*, 1625–1627.
[23] J. Jin, G. K. Soon, Y. Taekyung, C. Min, L. Jinwoo, Y. Jeyong, H. Taeghwan, *J. Phys. Chem. B* **2005**, *109*, 15297–15302.
[24] G. Guo, J. K. Whitesell, M. A. Fox, *J. Phys. Chem. B* **2005**, *109*, 18781–18785.
[25] W. Payakgul, O. Mekasuwandumrong, V. Pavarajarn, P. Praserthdam, *Ceram. Int.* **2005**, *31*, 391–397.
[26] G. Garnweitner, M. Antonietti, M. Niederberger, *Chem. Commun.* **2005**, 397–399.
[27] P. D. Cozzoli, A. Kornowski, H. Weller, *J. Am. Chem. Soc.* **2003**, *125*, 14539–14548.
[28] J. C. S. Wu, I. H. Tseng, W. C. Chang, *J. Nanopart. Res.* **2001**, *3*, 113–118.
[29] T. Trung, W. J. Cho, C. S. Ha, *Mater. Lett.* **2003**, *57*, 2746–2750.
[30] F. X. Perrin, V. Nguyen, J. L. Vernet, *J. Sol-Gel Sci. Technol.* **2003**, *28*, 205–215.
[31] H. P. Klug, L. E. Alexander, *X-ray Diffraction Precedures for Polycrystalline and Amorphous Materails*, 2nd ed., Wiley, New York, **1974**.
[32] T. Ohsaka, *J. Phys. Soc. Jpn.* **1980**, *48*, 1661–1668.
[33] T. Ohsaka, F. Izumi, Y. Fujiki, *J. Raman Spectrosc.* **1978**, *7*, 321–324.
[34] M. Gotic, M. Ivanda, S. Popovic, S. Music, A. Sekulic, A. Turkovic, K. Furic, *J. Raman Spectrosc.* **1997**, *28*, 555–558.
[35] C. Y. Xu, P. X. Zhang, L. Yan, *J. Raman Spectrosc.* **2001**, *32*, 862–865.
[36] Z. Zhang, X. Zhong, S. Liu, D. Li, M. Han, *Angew. Chem. Int. Ed.* **2005**, *44*, 3466–3470.
[37] U. Hwang, H. Park, K. Koo, *Ind. Eng. Chem. Res.* **2004**, *43*, 728–734.

Received: June 24, 2007
Published Online: January 15, 2008

